IL-1β Reduces Cardiac Lymphatic Muscle Contraction via COX-2 and PGE_2 Induction: Potential Role in Myocarditis

Mahmoud Al-Kofahi[*□], Seiichi Omura[†, #], Ikuo Tsunoda[†, #, §], Fumitaka Sato[†#]Felix Becker[*, ¶], Felicity N E Gavins[*, §], Matthew D. Woolard[†], Christopher Pattillo*, David Zawieja[Φ], Mariappan Muthuchamy[Φ], Anatoliy Gashev[Φ], Israa Shihab*, Mohammed Ghoweba,*, Pierre-Yves Von der Weid,[¥], Yuping Wang[*, ‡] and J. Steven Alexander[*, §]

[*]Department of Molecular & Cellular Physiology, [†]Department of Microbiology and Immunology, [‡]Department of Obstetrics and Gynecology, [§]Department of Neurology, Louisiana State University Health Sciences Center-Shreveport, Louisiana, [□] Department of Experimental and Clinical Pharmacology, College of Pharmacy, University of Minnesota, Minneapolis, Minnesota, [¶]Department for General and Visceral Surgery, University Hospital Münster, Germany, [#]Department of Microbiology, Kindai University Faculty of Medicine, Osaka, Japan, ¥Department of Pharmacology, University of Calgary, Alberta, Canada, [Φ]Texas A&M University, College Station, TX

Running Title: Cardiac lymphatic disturbances in myocarditis

Corresponding author:

J. Steven Alexander, PhD

Louisiana State University Health Sciences Center-Shreveport

Department of Molecular & Cellular Physiology

1501 Kings Highway, Shreveport, LA 71130

Email: jalexa@lsuhsc.edu

1 Tel: 318-675-4151, Fax: 318-675-4156

Abstract:

The role of lymphatic vessels in myocarditis is largely unknown, while it has been shown to play a key role in other inflammatory diseases. We aimed to investigate the role of lymphatic vessels in myocarditis using *in vivo* model induced with Theiler's murine encephalomyelitis virus (TMEV) and *in vitro* model with rat cardiac lymphatic muscle cells (RCLMC). In the TMEV model, we found that upregulation of a set of inflammatory mediator genes, including interleukin (IL)-1β, tumor necrosis factor (TNF)-αand COX-2 were associated with disease activity. Thus, using *in vitro* collagen gel contraction assays, we decided to clarify the role(s) of these mediators by testing contractility of RCLMC in response to IL-1β and TNF-α individually and in combination, in the presence or absence of: IL-1 receptor antagonist (Anakinra); cyclooxygenase (COX) inhibitors inhibitors (TFAP, diclofenac and DuP-697). IL-1β impaired RCLMC contractility dose-dependently, while co-incubation with both IL-1β and TNF-α exhibited synergistic effects in decreasing RCLMC contractility with increased COX-2 expression. Anakinra maintained RCLMC contractility; Anakinra blocked the mobilization of COX-2 induced by IL-1β with or without TNF-α. COX-2 inhibition blocked the IL-1β-mediated decrease in RCLMC contractility. Mechanistically, we found that IL-1β increased prostaglandin (PG) E_2 release dose-dependently, while Anakinra blocked IL-1β mediated PGE_2 release. Using prostaglandin E receptor 4 (EP4) receptor antagonist, we demonstrated that EP4 receptor blockade maintained RCLMC contractility following IL-1β exposure. Our results indicate that IL-1β reduces RCLMC contractility via COX-2/PGE_2 signaling with synergistic cooperation by TNF-α. These pathways may help provoke inflammatory mediator accumulation within the heart, driving progression from acute myocarditis into dilated cardiomyopathy.

Keywords: myocarditis, IL-1β, TNF-α, COX-2, PGE_2, lymphatic contractility

Abbreviations:

COX-1 = cyclooxygenase-1

COX-2 = cyclooxygenase-2

DCM = dilated cardiomyopathy

DMEM = Dulbecco's Modified Eagle Medium

ELISA = enzyme-linked immunosorbent assay

EP1 = prostaglandin E receptor 1

EP2 = prostaglandin E receptor 2

EP3 = prostaglandin E receptor 3

EP4 = prostaglandin E receptor 4

FBS = fetal bovine serum

HCl = hydrochloric acid

HF = heart failure

IACUC = Institutional Animal Care and Use Committee

ICM = ischemic cardiomyopathy

IFN-γ = interferon-gamma

IL-1β = interleukin-1 beta

LEC = lymphatic endothelial cells

LSUHSC-S = Louisiana State University Health Sciences Center-Shreveport

LYVE-1 = lymphatic vessel endothelial hyaluronan receptor 1

MI = myocardial infarction

NaOH = sodium hydroxide

NF-kB = nuclear factor kappa-light-chain-enhancer of activated B cells

PCA = principal component analysis

PGE_2 = prostaglandin E2

PTGER1 = prostaglandin E receptor 1 (subtype EP1)

PTGER2 = prostaglandin E receptor 2 (subtype EP2)

PTGER3 = prostaglandin E receptor 3 (subtype EP3)

PTGER4 = prostaglandin E receptor 4 (subtype EP4)

PTGS1 = prostaglandin-endoperoxide synthase 1

PTGS2 = prostaglandin-endoperoxide synthase 2

RCLMC = rat cardiac lymphatic muscle cells

TFAP = N- (5-Amino-2-pyridinyl)-4-trifluoromethylbenzamide

TMEV = Theiler's murine encephalomyelitis virus

TNF-α = tumor necrosis factor alpha

VEGFR3 = vascular endothelial growth factor receptor 3

VSMC = vascular smooth muscle cells

Introduction

Myocarditis is an inflammatory disease of the myocardium, which can be triggered by diverse infectious agents including bacteria, parasites, fungi but most commonly, viruses (1, 2). Myocarditis has been closely implicated with the pathogenesis of sudden death, dilated cardiomyopathy (DCM) and heart failure (HF) (3, 4). Despite many investigations revealing microvascular changes in myocarditis and DCM, research into the roles played by the lymphatic vasculature in such cardiopathies has been comparatively neglected (5).

The main function of the cardiac lymphatic system is to regulate interstitial fluid pressure, thus maintaining tissue homeostasis and preventing myocardial edema (6). The cardiac lymphatic system also plays an important role in immune surveillance and recovery following tissue injury in the heart (6). The cardiac lymphatic networks exist in all three layers of the heart wall with lymph flowing from endocardium through the myocardium to the epicardium and ultimately draining to the right lymphatic duct (7). Both “intrinsic” lymphatic contractions and “extrinsic” tissue compressive forces contribute to generate a sufficient pressure gradient acting to propel lymph centrally (8). To maintain a unidirectional lymph flow, lymphatic vessels have the intrinsic ability to propel lymph by spontaneous contractions within serially connected valve-containing contractile subunits, called ‘lymphangions’ (9). Simultaneously, lymphatic vessels exhibit tonic contraction that resembles the myogenic response in arterioles, which regulate lymphatic vessel diameter, and hence lymphatic vessel compliance and resistance (10, 11).

It has long been assumed that cardiac lymph flow depends only on external compressive forces generated during systole. During diastole, however, cardiac lymph flow may also reflect active contraction of lymphatics (12, 13), since cardiac lymph flow is maintained during conditions where cardiac contractility is impaired, e.g. myocardial ischemia, ventricular

fibrillation and during anoxic cardiac arrest, consistent with forms of lymph propulsion, independent of cardiac contraction (14-16).

Conversely, impaired cardiac lymph flow may participate in several forms of cardiac injury such as DCM and HF (17-19). Inflammatory responses in myocarditis include intense myocardial edema and formation of inflammatory infiltrates composed of lymphocytes and macrophages, both of which can be associated with an underlying lymphatic contraction disturbance (20, 21). Myocardial edema has been seen in several forms of cardiac inflammation, which is associated with increased myocardial lymph flow rate and decreased lymphatic outflow resistance (22). On the other hand, recent studies have shown that the contractile capacity of collecting lymphatics in other organs is often impaired in inflammatory diseases (23). Several other studies have also shown that inflammatory mediators can negatively regulate forms of lymphatic contraction (24-26).

Inflammatory cytokines, particularly interleukin (IL)-1 beta (β) and tumor necrosis factor (TNF)-α have been shown to be produced very early during viral myocarditis and persist throughout infection (27). High levels of plasma circulating IL-1β and TNF-α are found in patients with acute myocarditis, DCM and HF (28). In addition, some features of HF may arise, at least in part, from the toxic effects of endogenous cytokine cascades within the heart (29). Prolonged expression and accumulation of inflammatory cytokines play a role in driving the progression from acute myocarditis into DCM; failure of the cardiac lymphatic pump to clear inflammatory cells and cytokines in acute myocarditis may intensify accumulation of these cytokines, which exacerbates tissue damage, leading to DCM (30).

Previously, involvement of lymphatics has been investigated in terms of lymphangiogenesis, rather than the functional changes in pre-existing lymphatics. In another

form of cardiac injuries, myocardial infarction (MI), lymphatic vessel density was increased in the peri-infarction area 2 weeks after MI in experimental mouse model. This lymphatic remodeling was also accompanied by high levels of lymphangiogenic factors such as VEGF-C and D, Prox-1, and LYVE-1 (49). Further studies have shown that cardiac lymphatics undergo significant lymphangiogenesis in response to myocardial injury in an experimental mouse model of MI (50). VEGF-C-treated mice exhibited neo-lymphangiogenesis, which significantly improved cardiac function and prognosis after MI (50). On the other hand, there are only a few reports on lymphatic vessels and lymphangiogenic responses in DCM and myocarditis (19). One report showed no difference in lymphatic density in patients with chronic Chagasic (Chagas disease mediated) cardiomyopathy that was characterized by the presence of chronic lymphohistiocytic myocarditis, compared to control group (51). Others showed increased lymphatic biomarkers in ischemic cardiomyopathy (ICM) and DCM, but with different patterns of the expression of these markers suggesting distinctive forms of lymphatic remodeling that may reflect influences of chronic myocardial interstitial edema (22, 52). However, to what extent such lymphangiogenesis may function as a compensatory mechanism to maintain tissue homeostasis and reduce tissue edema and remodeling in myocarditis and DCM is unknown (19).

While lymphatic contractility has been studied extensively in organs other than the heart, i.e. intestine, far less is known about cardiac lymphatic muscular contraction and its involvement in myocarditis (31). Thus, in the current experiments, we first demonstrated the increased expression levels of inflammatory mediators and lymphatic biomarker genes in hearts *in vivo* during acute viral myocarditis induced with Theiler's murine encephalomyelitis virus (TMEV). Then, we tested how inflammatory cytokines could affect tonic contraction of rat cardiac lymphatic smooth muscle cells (RCLMC) *in vitro*. Here, we have for the first time demonstrated

that inflammatory cytokines, associated with myocarditis pathophysiology, have a profound depressive effect on cardiac lymphatic tonic contractility and these events appear to involve cyclooxygenase-2 (COX-2)/prostaglandin E2 (PGE_2) signaling.

Materials and Methods

Ethical approval

All animal handling and experimental procedures involving the use of animals were reviewed and approved by the Institutional Animal Care and Use Committee (IACUC) of Louisiana State University Health Sciences Center-Shreveport (LSUHSC-S) and were in accordance to the National Institutes of Health guide for the care and use of laboratory animals.

Experimental murine acute viral myocarditis

Male 5-week-old C3H/HeN mice (Taconic Farms, Hudson, NY) were used and maintained on 12/12-hour (h) light/dark cycles in standard animal cages with filter tops under specific pathogen-free conditions in the animal care facility at LSUHSC-S. Mice were given standard laboratory rodent chow and water *ad libitum*. For induction of acute viral myocarditis, 5-week-old mice were infected with 2×10^7 plaque forming units (PFUs) of the Daniels (DA) strain of TMEV-intraperitoneally, as we described previously (32, 33). Age-matched uninfected mice were used as controls. Mice were monitored and weighed daily. On 7 days post infection (dpi), five mice per group were anesthetized (isoflurane, Vedco, Saint Joseph, MO), and subsequently sacrificed for cardiac tissue collection.

Myocardial gene expression

Hearts were homogenized in TRI Reagent® (Molecular Research Center, Cincinnati, OH), using the Kinematica PolytronTM homogenizer (Kinematica, Bohemia, NY) (32). Total RNA was extracted from homogenates, using the RNeasy Mini Kit (Qiagen, Valencia, CA), and

DNase treatment was performed during RNA isolation, using the RNase-Free DNase Set (Qiagen). All samples were purified to an absorbance ratio (A260/A280) between 1.9 and 2.1.

For labeled cDNA fragments, 100 ng of total RNA were converted using Poly-A RNA Control (Affymetrix, Santa Clara, CA), Ambion® WT Expression Kit (Life Technologies Corporation, Carlsbad, CA), and Affymetrix proprietary DNA Labeling Reagent (Affymetrix) (34). Labeled cDNA fragments were hybridized to the GeneChip® Mouse 1.0ST Array (Affymetrix) that includes 28,853 transcripts. Hybridized arrays were washed and stained using the GeneChip® Hybridization Wash and Stain Kit (Affymetrix) and the GeneChip® Fluidics Station 450 (Affymetrix), and scanned using the GeneChip® Scanner 3000 (Affymetrix). Data were visualized and quantified by the Affymetrix GeneChip® Command Console (AGCC), and normalized by Robust Multi-array Average (RMA), using Expression Console™ (Affymetrix). Fold changes were calculated as ratios of signal value, compared with age-matched controls. Log ratios were calculated by the logarithm of fold changes to base 2. Microarray results were analyzed using the Ingenuity Pathway Analysis® (IPA, Ingenuity Systems, www.ingenuity.com), NetAffx database (Affymetrix, www.affymetrix.com/index.affx), and Mouse Genome Informatics (Jackson Laboratory, Bar Harbor, ME, www.informatics.jax.org/). The data have been deposited into the Gene Expression Omnibus (GEO) repository in National Center for Biotechnology Information (NCBI) (Accession number: GSE53607) (32).

Principal component analysis (PCA)

Among the transcription data, we selected 12 genes / samples, which have been described as key inflammatory molecules and lymphatic markers. PCA can reduce the dimensionality of a data set consisting of a large number of interrelated variables, while retaining as much as

possible of the variation present in the data set (35). PCA was conducted as an “unsupervised” analysis to test whether the variance of the 12 gene expression levels among the 10 heart samples could separate five infected versus five control samples as distinct groups, using a Q-mode PCA package ‘prcomp’ of R (36). We also calculated the proportion of variance of each principal component (PC) and factor loading for PC1, the latter of which enable us to rank the 12 genes based on positive or negative contribution to PC1 values, as we described previously (32, 33, 37).

Rat cardiac lymphatic muscle cells (RCLMC) isolation and preparation

RCLMC were isolated from freshly excised hearts collected from healthy adult Sprague-Dawley rats (Charles River Laboratories, Charleston, SC). The ventricular epicardial surface was superficially injected with 5 µl of lymphazurin (1% isosulfan blue, Covidien, New Haven, CT) and sterilely incubated at 37°C for 45 minutes (min) at 100% humidity. Epicardial lymphatic vessels visualized by this approach were excised, dissected and then washed extensively with Dulbecco's Modified Eagle Medium (DMEM) supplemented with 10% fetal bovine serum (FBS) and 3% antibiotic/antimycotic. Tissue fragments were incubated in 0.2% collagenase (type II, Worthington) in DMEM at 37°C for 2 hours (h). Cells were collected by centrifugation at 485 x *g* and seeded onto tissue culture plate, where islands of cells attached within 24 h. To remove potential endothelial cell contaminants, confluent third passage (P3) RCLSMC cultures were treated with 50 mM L-leucine methyl ester (LLME, Synthetech, Albany, OR) for 2 h in DMEM supplemented with 10% FBS, 1% antibiotic/antimycotic and glutamine (supplemented DMEM) (38). Adherent cell cultures were rinsed three times with supplemented DMEM and cultures

maintained in supplemented DMEM. Cultures reached a confluent density of 80,000 cells/cm^2 and showed no reduction in proliferation over at least 12 passages.

Unlike lymphatic endothelial cells (LEC), lymphatic muscle cells lack any specific marker that differentiate them from vascular smooth muscle cells (VSMC). However, Muthuchamy *et al.* have shown that different types of smooth muscle express various forms of smooth muscle (SM) myosin heavy chains (MHC) and their function can be explained based on the relative content of various SM MHC isoforms (39). Thus, we examined the relative content of various SM MHC (SM A/B and/or SM 1/2) in our isolated cells to further confirm their lymphatic origin. Reverse transcription-polymerase chain reaction (RT-PCR) was used to define and measure possible SM MHC isoforms mRNA expression in RCLMC. As previously described by Muthuchamy *et al.* and similar to isolated cultured rat mesenteric lymphatic muscle cells, RCLMC also expressed SMA and SM1 isoforms of MHC, but not SMB or SM2 (data not shown) (39).

Collagen gel contraction assay

Type 1 collagen matrices were prepared as we previously described (26). Type I collagen was prepared by stirring 100% isopropanol (Thermo/Fisher) -washed adult rat-tail tendons for 48 h at 4°C in sterile 4 mM acetic acid under constant agitation. After filtration through a 250 μm nylon filter (Spectrum Labs, Rancho Dominguez, CA), solubilized type I collagen solution was centrifuged at 19 x *g* for 20 min at 4°C, aliquoted and stored at -20°C. Frozen aliquots were then freeze dried using a bench-top manifold freeze-dryer (Millrock Technology, Kingston, NY), and stored at -20°C for future use.

On the day prior to experiments, dried collagen was dissolved in cold 0.012 M HCl at final concentration of 2.5 mg/ml, mixed gently (to avoid introducing bubbles) on a rocker at 4°C overnight until all collagen re-dissolved into a gel (0.1% type I collagen gels). On the day of experiments, RCLMC were harvested with trypsin-EDTA (Sigma-Aldrich), and a total of $1.2x10^6$ cells were re-suspended in 8 ml of supplemented DMEM, incorporated into 3.2 ml of 0.1% type I collagen gels. Next, 0.8 ml of 5x PBS and 5 μl 0.5 M NaOH was added to the RCLMC/type 1 collagen gel mix bringing the total volume to 12 ml. Lastly, 500 μl aliquots of the RCLMC/type 1 collagen gel mixture were seeded in into 24 well plates (Thermo/Fisher) and incubated at 37°C for 1 h to polymerize (26).

Cytokine treatment and gel contraction image analysis

After polymerization, RCLMC were incorporated into 0.1% type I collagen gels at 50,000 cells/well and treated with 1 ml supplemented DMEM containing: recombinant human IL-1β (5, 10 and 20 ng/ml, Thermo/Fisher, Waltham, MA), recombinant human TNF-α (20 ng/ml, Thermo/Fisher, Waltham, MA), with or without COX inhibitors, COX-1 inhibitor IV N-(5-Amino-2-pyridinyl)-4-trifluoromethylbenzamide (TFAP) 10^{-5} M (EMD Millipore**,** Billerica, MA), diclofenac Na $0.2x10^{-5}$M (Sigma-Aldrich), DuP-697 (Cayman Chemical, Ann Arbor, MI), PGE_2 10^{-5}M (Cayman Chemical), IL-1 receptor antagonist, Anakinra 5 μg/ml (Kineret®, Sobi, Inc., Ardmore, PA) or prostaglandin E receptor 4 (EP4) antagonist GW627368X 10^{-6}M and 10^{-7}M (Cayman Chemical). All RCLMC/gels were then gently detached from the edges of the plates, and incubated for 4 days at 37°C in 7.5% CO_2.

Changes in RCLMC tonic contraction were monitored and digital photographs were recorded daily over 4 days using a camera (Nikon D40, Tokyo, Japan). At least five different

culture of RCLMC were used to perform every single experiment and each culture was used to set up a minimum of 4 replicates (wells) per treatment dosage. The average of RCLMC contraction for each treatment dosage were calculated as the average of RCLMC in four wells and represent a single n-value, the experiment was repeated five times. All experimental conditions and treatment doses were previously optimized based on our previously published work (26). Gel contraction was measured as the change in gel surface area on day 4 as a fraction of its area measured on day 0, and normalized to internal controls, as described previously (26).

Western blotting

RCLMC were seeded in 6-well plates at 37°C in 7.5% CO_2 and incubated until fully confluent. RCLMC were treated with supplemented DMEM alone (control) or supplemented DMEM plus IL-1β (20 ng/ml), TNF-α (20 ng/ml), IL-1β (20 ng/ml) + TNF-α (20 ng/ml), IL-1β (20 ng/ml) + Anakinra (5 μg/ml) or IL-1β (20 ng/ml) + TNF-α (20 ng/ml) + Anakinra (5 μg/ml). After 24 h, RCLMC were washed twice with PBS, collected in 100 μl reducing sample buffer (45% Milli-Q water, 12% 0.5 M Tris-HCl, pH 6.8, 2% sodium dodecyl sulfate (SDS), 15% glycerol, 2% phenol red, Sigma-Aldrich)), 10% β-mercaptoethanol and protease inhibitor cocktail (Sigma-Aldrich), sonicated, boiled for 1 min at 100°C and stored at -80°C.

After measuring total protein concentration (660 nm Protein Assay, Thermo/Fisher), 40 μg protein of each RCLMC lysate was subjected to electrophoresis on 7.5% SDS-polyacrylamide gels and transferred to nitrocellulose membranes using a transblot apparatus (Idea Scientific Minneapolis, MN). Membranes were stained with Ponceau-S (Sigma-Aldrich) to verify protein transfer, blocked overnight at 4°C with 5% non-fat milk and were incubated with anti-COX-2 antibody (Cayman Chemical, 1:1,000 in 0.1% milk powder). Membranes were incubated for 1 h

at room temperature (RT) before adding anti-rabbit IgG (whole molecule)-peroxidase antibody (Sigma-Aldrich, 1:1,500 in 0.1% milk) as a secondary antibody for 1 h at RT. Enhanced chemiluminescence (Pierce ECL Western Blotting Substrate, Rockford, IL) was used to visualize the blots, and the density of resulting bands measured using NIH Image-J analysis program (40).

PGE_2 ELISA

RCLMC were cultured in 6-well plates and incubated at 37°C in 7.5% CO_2 until fully confluent. Medium was replaced with supplemented DMEM alone (control) or with IL-1β (5, 10, 20 ng/ml), TNF-α (20 ng/ml) or IL-1β (20 ng/ml) + Anakinra (5 μg/ml). At 24 h, supernatants were collected and stored at -80°C. PGE_2 concentrations were measured in supernatants using a PGE_2 ELISA kit (ENZO Life Science® Farmingdale, NY), according to manufacturer's instructions.

Immunofluorescent staining of cardiac lymphatics

Cardiac lymphatics and smooth muscle were visualized using immunofluorescence for alpha-smooth muscle actin and lymphatic vascular endothelial hyaluronic acid receptor-1 (LYVE-1). We embedded rat hearts in paraffin and made 5-μm thick sections. Antigen retrieval was carried out in unmasking solution and heating in a pressure cooker for 20 min. After cooling to room temperature for 20 min, slides were washed with deionized water (twice, 5 min) with gentle shaking. Slides were blocked with 5% goat serum (diluted with 1% milk in PBS) for 30 min and washed again with deionized water twice for 5 min. Primary antibodies (rabbit anti-LYVE-1, diluted 1:75), α-smooth muscle actin (SMA) (diluted 1:250) were prepared in 1% milk in PBS and 100 μl added to each slides and incubated overnight at 4°C. Secondary antibodies

FITC anti-rabbit (in donkey, dilution 1:250) and TRITC anti-mouse (donkey, diluted 1:250), were added to slides. Slides were mounted in DAPI mounting medium.

Statistical analysis

Data are presented as mean ± standard error of the mean (SEM). Table 1 data analyses were determined using the paired two-tailed Student's *t*-test. Statistical analyses (GraphPad Software, Inc., La Jolla, CA) were performed using one-way ANOVA with Bonferroni test as post-hoc test. Comparisons were considered statistically significant at $p < 0.05$.

Results

LYVE-1 and SMA dual positive lymphatic vessels are abundant in the heart.

Since dual immunofluorescence for LYVE-1 with SMA can visualize muscular lymphatic and non-lymphatic vessels in the myocardium, we detected muscular lymphatic vessels that are dual positive for LYVE-1 and SMA in the myocardium by immunofluorescence to evaluate the possible significance of these vessels in myocardial biology. **Figure 1** shows dual stained muscular lymphatic vessels (yellow and yellow arrows, lower right panel) which were distinct from LYVE-1^{-}/SMA^{+} (red) vessels, and distinct from non-muscularized lymphatics (green and green arrows, lower right panel) (DAPI nuclear staining is shown in **Figure 1**, lower left). While lymphatics in the mammalian heart are well known to contribute to normal cardiac structure function, these muscular cardiac lymphatic vessels may fulfill important functions in the control of interstitial balance in the heart.

Inflammatory mediators have been shown to contribute to the pathophysiology of human and experimental myocarditis (27, 28). We have previously determined gene expression profiles in hearts of mice with viral myocarditis (32). Here, we used transcriptome data to compare expression levels of inflammatory mediators and lymphatic marker genes in hearts from TMEV-infected mice with acute viral myocarditis (7 dpi) using pairwise comparison (**Table 1**). We found significant upregulation of several inflammatory mediator genes, including IL-1β, TNF-α, COX-2 and EP4 receptor and down regulation of COX-1. On the other hand, significant changes in the lymphatic markers LYVE-1 and VEGFR3 were not observed. We have previously documented the induction of viral myocarditis in these mice using the TMEV model which is described in Omura et al. (66).

PCA of inflammatory mediators and lymphatic markers distinguishes between control and myocarditis mice

To determine whether a set of inflammatory mediators and lymphatic markers could distinguish mice with myocarditis from controls, we conducted PCA, using transcriptome data of 12 genes, shown in **Table 1**, in the hearts from control and myocarditis mice (total 10 samples). In PCA, each principal component (PC) is defined in an unsupervised manner, depending on the variance of 12 gene expression levels among the 10 samples. We found that samples were separated clearly into two distinct groups, control and myocarditis groups, based on PC1 values **(Figure 2A)**. The proportions of variance of PCs showed that PC1 explained 54% of the variance among 10 samples **(Figure 2B)**. To rank what genes contributed to the PC1 value, we determined a factor loading for PC1. We found that the gene expression levels of three pro-inflammatory cytokines [IL-1β, interferon (IFN)-gamma (γ), and TNF-α], IL-1 receptor 1, and three other molecules: prostaglandin E receptor 2 (EP2), EP4 and COX-2 contributed to PC1 distribution positively, while five gene expression levels, particularly COX-1, and lymphatic markers (LYVE-1 and VEGFR3) contributed to PC1 distribution negatively **(Figure 2C)**.

IL-1β dose-dependently decreases RCLMC tonic contractility, while IL-1β receptor antagonist Anakinra maintains RCLMC contractility

Among the molecules examined above *in vivo*, IL-1β and TNF-α have been shown to be increased during acute viral myocarditis (27), we tested whether these inflammatory mediators would influence cardiac lymphatic muscle tonic contractility using our *in vitro* collagen gel contraction assay (26). IL-1β-treated gels exhibited significantly impaired RCLMC tonic contractility compared with control at 4 dpi (79.8±2.1% vs. control, *** $p < 0.001$) (**Figure 3A**),

while TNF-α alone had no effect on RCLMC contractility. To evaluate possible synergistic interactions between IL-1β and TNF-α, we studied combined effects of TNF-α + IL-1β on RCLMC tonic contractility, and found a significantly enhanced relaxation compared with IL-1β alone (66.3±4% vs. control, *** $p < 0.001$) (TNF-α + IL-1β vs. IL-1β, # $p < 0.001$). Further, we tested different doses of IL-1β, and found a dose dependent effect of IL-1β on RCLMC contractility [5 ng/ml (91.1±2.2%, * $p < 0.05$), 10 ng/ml (88.3±1.2%, ** $p < 0.01$) and 20 ng/ml (81.6±2%, *** $p < 0.001$) vs. control (20 ng/ml vs. 10 ng/ml # $p < 0.05$, 20 ng/ml vs. 5 ng/ml $ $p < 0.01$)] (**Figure 3B**).

We next tested if Anakinra could reverse the relaxation effect of IL-1β on RCLMC. When co-treated with Anakinra, RCLMC tonic contractility was $p > 0.99$) as well as IL-1β + TNF-α treated gels compared with control at 4 dpi (97.5±2.1% vs. control, $p > 0.99$) (**Figure 3A**).

IL-1β and IL-1β + TNF-α increase COX-2 protein levels in RCLMC, while Anakinra inhibits IL-1β-induced COX-2 expression.

In our *in vivo* experiments, we also found increased COX-2 expression in the heart from acute viral myocarditis (**Table 1**). Previous studies, including our own, have shown that IL-1β increases COX-2 protein levels in vascular, bronchial and mesenteric lymphatic smooth muscle (26, 41, 42). To test whether IL-1β induces the same effect in RCLMC, we examined the effect of inflammatory cytokines on COX-2 protein expression levels. IL-1β-treated RCLMC showed a nearly a 10-fold increase in COX-2 protein levels: density values (arbitrary unit) = IL-1β, 154,152±26,313 vs. control, 15,240±4,927, ** $p < 0.01$, while TNF-α had no effect on COX-2 levels. To test whether the synergy between IL-1β and TNF-α that decreased contractility of

RCLMC was related to increased COX-2 protein expression; we tested the effect of these cytokines in combination on RCLMC COX-2 expression. IL-1β + TNF-α induced 30-fold higher levels of COX-2 compared with controls (IL-1β + TNF-α, 440,828±36,957 vs. control, 15,240±4927, *** $p < 0.001$) and about 3-fold higher levels than IL-1β alone (IL-1β, 154,152±26,313, # $p < 0.001$). Again, Anakinra blocked the increased level of COX-2 induced by IL-1β or IL-1β + TNF-α (**Figure 4 A and B**).

COX-2 inhibition blocks IL-1β-induced RCLMC relaxation.

To test whether IL-1β-induced RCLMC relaxation depends on COX-2, we tested the effect of a selective COX-1 inhibitor (COX-1i = TFAP), a nonselective COX-1 and 2 inhibitor (COX-1/2i = Diclofenac) or a selective COX-2 inhibitor (COX-2i = Dup-697) on IL-1β-induced RCLMC relaxation. RCLMC/collagen gels were treated with either control media, IL-1β, IL-1β + COX-1 inhibitor, IL-1β + COX-1/2 inhibitor or IL-1β + COX-2 inhibitor. We found that COX-2 inhibition by both the nonselective COX-1/-2 inhibitor (diclofenac) (96.3±1.8% vs. control, $p > 1.0$) and the selective COX-2 inhibitor (Dup-697) (103.6±1.4% vs. control, $p > 1.0$) blocked the IL-1β-induced RCLMC relaxation, maintaining RCLMC at the same levels of contraction as controls (**Figure 5A**). On the other hand, the selective COX-1 inhibitor had no effect on IL-1β-induced RCLMC relaxation (79.4±5.2% vs. control, ** $p < 0.01$). Treatment with none of these COX inhibitors alone showed any direct effects on RCLMC tonic contraction (**Figure 5B**).

IL-1β dose dependently induces PGE_2 production in RCLMC, while IL-1β receptor blockade inhibits PGE_2 production.

In vascular, bronchial and mesenteric lymphatic smooth muscle cells, IL-1β has been shown to potently induce a vasodilator PGE_2 (26, 41, 42). To test whether IL-1β could induce PGE_2 production in RCLMC, we quantified PGE_2 in supernatants of RCLMC following treatment with IL-1β, TNF-α or IL-1β + Anakinra. IL-1β significantly increased PGE_2 levels in a dose dependent fashion compared with control: 20 ng/ml, 1,152±141 pg/ml, *** $p < 0.001$; 10 ng/ml, 849±22 pg/ml, ** $p < 0.001$; and 5 ng/ml, 412±17 pg/ml, * $p < 0.001$; vs. control, 81.6±3.1 pg/ml (20 ng/ml vs. 10 ng/ml # $p < 0.05$, 5 ng/ml vs. 10 ng/ml, $ $p < 0.01$) (**Figure 6A**), while Anakinra blocked PGE_2 induction in RCLMC treated with IL-1β (50±9 pg/ml vs. control 82±3 pg/ml, $p > 0.99$). TNF-α had no significant effect on PGE_2.

EP4 receptor antagonist blocks IL-1β-induced RCLMC relaxation, while PGE_2 induces RCLMC relaxation.

To examine whether the PGE_2 receptor EP4 was required for IL-1β-induced RCLMC relaxation, we treated RCLMC with IL-1β + the EP4 receptor antagonist (GW627368X, 10^{-7}M and 10^{-6}M). We found that EP4 receptor blockade prevented IL-1β-induced RCLMC relaxation (95.4±0.8% and 94.8±1.8% vs. control, $p = 0.327$ and $p = 0.186$, respectively) (**Figure 6B**). Lastly, to test whether PGE_2 by itself could induce RCLMC relaxation; we treated RCLMC with exogenous PGE_2. We found that PGE_2 induced RCLMC relaxation (82.9±1.78% vs. control, ** $p < 0.01$). Anakinra showed no significant effect on PGE_2-induced RCLSMC relaxation.

Discussion

Clinical and experimental studies in viral myocarditis have shown that, in addition to injury of the myocardium by immune cell infiltrates, vascular dysfunction and vasospasm also contribute to the progression of viral myocarditis into DCM (43-46). However, it remains unknown whether and how cardiac lymphatic dysfunction might contribute to the pathophysiology of myocarditis.

During the early acute phase of murine viral myocarditis (0 to 3 dpi), Shioi *et al*. reported increased mRNA signatures for several different inflammatory cytokines, especially IL-1β and TNF-α, have been reported within the ventricular myocardium (27). Other reports have shown high protein levels of these cytokines, which were persistently expressed during acute/subacute (4 to 14 dpi) through chronic (15 to 90 dpi) phases of murine viral myocarditis (27, 47, 48).

Our data (**Table 1**) show that the cardiac gene expression of IL-1β and TNF-α were significantly elevated during the acute phase of viral myocarditis (7 dpi). Moreover, gene expression of COX-2, (also known as PTGS2), and the G-protein-coupled receptor EP4 prostanoid receptor, (also known as PTGER4) were significantly elevated in acute myocarditis. Using PCA, we demonstrated that mice with myocarditis could be distinguished from control mice using expression patterns of pro-inflammatory molecules and lymphatic markers, suggesting that this set of molecules potentially contribute to the etiology of myocarditis and may represent important and predictive biomarkers for this condition (**Figure 2**).

In the current experiments, although we found a potent induction of several inflammatory mediator genes including, IL-1β and TNF-α during acute experimental viral myocarditis, expression for mRNAs for lymphatic markers, LYVE-1 and VEGFR3 did not show significant changes compared with control. Since immune cell infiltration in TMEV-induced myocarditis has been shown to be active and progressive by 7 dpi, cardiac lymphangiogenic responses may

be absent or depressed at early stage of acute viral myocarditis (32, 33). Our in vivo myocarditis model did not support a role of lymphangiogenesis (i.e. no increases in lymphatic gene expression, (see results section)) which directed us to study the roles which may be played by lymphatic muscle cells.

In addition to the possibility of inefficient induction of lymphangiogenic responses in acute viral myocarditis (50), inflammatory mediators may depress contractility of cardiac lymphatics to further negatively influence lymph transport. Hence, stimulation of lymphangiogenesis and/or enhancement of lymph vessel propulsion may help compensate for low transport capacity per vessel to restore the myocardial lymph flow rate and relieve edema in myocarditis (22). Previously, we demonstrated that inflammatory cytokines, IL-1β and TNF-α, which are elevated in murine colitis and inflammatory bowel disease, induced profound LEC dysfunction, and also reduced mesenteric lymphatic muscle cell tonic contractility (26, 53).

In the current study, we examined effects of inflammatory cytokines, in particular IL-1β and TNF-α, on RCLMC tonic contractility. IL-1β significantly impaired RCLMC tonic contractility in a dose-dependent fashion, while TNF-α alone had no effect (**Figure 2**). We then studied the combined effect of TNF-α and IL-1β on RCLMC tonic contractility, compared with IL-1β alone. We found that, although TNF-α had no direct effect on RCLMC contractility, TNF-α did significantly potentiate the "relaxing" effect of IL-1β (**Figure 3A**). This indicates that synergy exists between IL-1β and TNF-α in the depression of RCLMC tonic contractility, but does not rule out the effect of other cytokines being involved in these responses. Moreover, previous studies have reported that IL-1β-mediated VSMC relaxation effect in a dose-dependent fashion, or acted synergistically with TNF-α to induce VSMC relaxation (54, 55).

IL-1β is one of the major cytokines predictive of poor outcomes in myocarditis (27). Clinical trials in patients with rheumatoid arthritis have shown that Anakinra, a recombinant form of IL-1 receptor antagonist, (IL-1RA) a blocking-'decoy' agonist of the IL-1 receptor (67) had beneficial effects on cardiac health measured by its ability to prevent restenosis, improve endothelial function, maintain coronary flow and left ventricular function (56-59). Further, IL-1 receptor blockade (using IL-1 receptor antagonist gene therapy) was shown effective at improving the survival rate in murine model of myocarditis induced with encephalomyocarditis virus (EMCV) (60). Based on our observations, we speculated that the protective effect by IL-1 receptor blockade in myocarditis may be at least partially due to maintenance of cardiac lymphatic contractility. To understand the potential contribution of IL-1β in such pathologies, we then tested how IL-1β blockade using Anakinra would affect RCLMC tonic contractility following challenge with either IL-1β alone or TNF-α + IL-1β (**Figure 3A**). Pharmacological inhibition of IL-1 receptor activity using Anakinra maintained RCLMC contractility following treatment with IL-1β alone or TNF-α + IL-1β in combination. These results suggest that IL-1β represents a major 'relaxant' cytokine and that TNF-α can potently intensify effects of IL-1β, since Anakinra also blocked the synergistic effect.

In acute viral myocarditis, cardiac tissue also produces substantial amounts of both COX-2 and COX-2 products, e.g. PGE_2 (61). IL-1β is known to be a potent inducer of COX-2 in both vascular and lymphatic muscle cells, as well as in virally infected macrophages (26, 41, 62). Since we found induction of both IL-1β and COX-2 gene expression in acute myocarditis *in vivo*, we studied the effect of IL-1β on COX-2 protein induction in RCLMC *in vitro*. We found that IL-1β increased COX-2 expression in RCLMC, while TNF-α alone had no effect. TNF-α combined with IL-1β induced a greater increase in COX-2 levels than IL-1β alone, while

Anakinra prevented the increased expression of COX-2 induced by either IL-1β or IL-1β+TNF-α (**Figure 4**). These results further support the concept of synergy between IL-1β and TNF-α in decreasing RCLMC tonic contractility, acting via higher-induction of COX-2 expression mediated by cumulative IL-1β and TNF-α signaling. Moreover, COX-2 inhibition using either the non-selective COX inhibitor diclofenac or the selective COX-2 inhibitor DuP-697 blocked IL-1β-induced RCLMC relaxation. On the other hand, COX-1 inhibition, using the selective COX-1 inhibitor TFAP, had no effect (**Figure 5A**). These results show that IL-1β-induced RCLMC relaxation *in vitro* depends on COX-2.

In our previous study, we demonstrated that IL-1β markedly increased PGE_2 synthesis by mesenteric lymphatic muscle cells (26). Furthermore, previous studies have shown that IL-1β mediates PGE_2 production in vascular and bronchial smooth muscle in an endothelial independent fashion (42, 63). Thus, we tested the effect of IL-1β on PGE_2 production in RCLMC. PGE_2 was markedly induced by IL-1β, but not by TNF-α alone, in a dose dependent fashion, while the induction of PGE_2 was prevented by Anakinra (**Figure 6A**). Then, we tested whether direct PGE_2 stimulation could decrease RCLMC tonic contractility as was similarly found for IL-1β. PGE_2 reduced RCLMC contractility similar to IL-1β; indicating that IL-1β induced PGE_2 production from RCLMC could potentially mediate RCLMC relaxation in an autocrine fashion, independent of endothelial cells (**Figure 6B**). We next tested the effect of the EP4 receptor antagonist GW627368X on IL-1β-induced RCLMC relaxation. GW627368X blocked IL-1β-induced RCLMC relaxation, suggesting that IL-1β could induce PGE_2 production, which acts in an autocrine fashion to decrease RCLMC tonic contractility via EP4 stimulation (**Figure 6B**).

Our present study reveals that inflammatory cytokines, especially IL-1β, can exert a profound depressant effect on cardiac lymphatic muscular contractility via COX-2 mediated PGE_2 production and EP4 receptor activation to inhibit RCLMC tonic contraction. This pathway may also involve phenotypic transition in RCLMC, as IL-1β has shown to be the only inflammatory cytokine to trigger this phenotypic transition of vascular smooth muscle cells from contractile to stellate cells (63). This trans-differentiation process has also been shown to involve reduction in the expression of contractile proteins and disruption of focal adhesions and actin stress fiber organization in response to the autocrine/paracrine secretion of PGE_2 and EP4 activation (63).

Although the diameter of cardiac lymphatic vessels has never been examined in myocarditis, increased lymphatic vascular diameter has shown to increase proportionally with the severity of inflammation in other inflammatory diseases (23). Thus, the loss of cardiac lymphatic tonic contractility induced by IL-1β seen in our current study, could reflect lymphostasis and vessel dilation. Within non-contracting but valve bounded collecting lymphatics, vessel tone may also maintain a sufficiently constricted vascular radius, which permits appropriate apposition of lymphatic valve leaflets, which establish and maintain unidirectional lymphatic flow. It is also possible that if a sufficient level of tonic vessel contraction is not maintained, normal valve sealing may not occur leading to lymph stasis or reflux. Thus, while probably not directly participating in the active propulsive lymph transport, tonic lymphatic muscle contraction nerveless may play important roles in maintain a functional and unidirectional lymph transport (64). Therefore, the loss of cardiac lymphatic tonic contractility induced by IL-1β would exacerbate myocardial edema leading to accumulation of

inflammatory mediators and immune cells within the heart which is described schematically in **Figure 7.**

The current study has defined molecular mechanisms that might underlie in myocarditis pathophysiology. The relaxing effect of IL-1β on cardiac lymphatics may provide a novel mechanism linking IL-1β to reported poor clinic outcomes in myocarditis, and help identify strategies to prevent progression from acute myocarditis to DCM, although further studies are necessary to better understand potential roles of the cardiac lymphatic system in the etiology of myocarditis and to determine the extent to which lymphatic failure drives progression of myocarditis into DCM. In summery our current results provided crucial mechanistic and translational insights that may help exploit lymphatics as novel targets for therapeutic management of myocarditis (65).

Funding

This work funded by a graduate research fellowship from the Center for Cardiovascular Diseases and Sciences, LSU Health Science Center-Shreveport (M. Al-Kofahi, F. Sato and S. Omura), a grant from the Department of Defense (W81XWH-11-1-0577, J.S. Alexander), the German Research Foundation (DFG, BE 5619/1-1, F. Becker), the National Institute of General Medical Sciences of the National Institutes of Health (NIH Award P30GM110703, I. Tsunoda), the Science Research Promotion Fund from the Promotion and Mutual Aid Corporation for Private Schools of Japan (F. Sato), the Faculty Assistance and Development Research Grants from the Kindai University Research Enhancement Grant (F. Sato and S. Omura), the KAKENHI from the Japan Society for the Promotion of Science (JP17K15628, F. Sato; and JP16H07356, I. Tsunoda), and NIH/NHLBI (ML125572-01A1, F.N.E. Gavins).

Figure legends

Figure 1. Immunolocalization of muscular, non-muscular lymphatics and blood vessels in the heart. Figure 1 shows dual stained muscular lymphatic vessels (shown by yellow staining and yellow arrows, lower right panel) which were distinct from LYVE-1^{-}/SMA^{+} (red staining and red arrows) blood vessels, and from non-muscularized collecting lymphatics (green and green arrows, lower right panel). DAPI nuclear staining is shown in lower left panel.

Figure 2. Principal component analysis (PCA) of mRNA levels of 12 key pro-inflammatory and lymphatic markers selected from transcriptome data of the hearts from Theiler's murine encephalomyelitis virus (TMEV)-infected mice with myocarditis. **A)** PCA separated clearly between the mice with viral myocarditis versus control mice, based on principal component (PC) 1. **B)** PC1 explained 54% of variance among the mouse heart samples. **C)** Gene expression levels of seven pro-inflammatory [interferon (IL)-β, interferon (IFN)-γ, and tumor necrosis factor (TNF)-α], IL-1 receptor 1, and receptors [prostaglandin E receptors (EP2 and EP4) and cyclooxygenase (COX)-2] contributed to PC1 distribution positively, while five gene expression levels, particularly, COX-1 and vascular endothelial growth factor receptor (VEGFR) 3, contributed negatively. PCA was conducted using an R package 'prcomp'. Five mice per group were used and the hearts were harvested on 7 days post infection (dpi).

Figure 3. IL-1β dose-dependently decreased rat cardiac lymphatic muscle cells (RCLMC) tonic contractility. **A)** IL-1β significantly decreased RCLMC tonic contractility compared with controls. TNF-α alone (20 ng/ml) produced a slight relaxation which was not significant compared to controls. TNF-α did significantly enhanced the relaxing effect of IL-1β on RCLMC

compared with IL-1β alone. Anakinra maintained RCLMC tonic contractility in the presence of IL-1β or IL-1β -+ TNF-α at day 4. n= 6, *** $p < 0.001$ vs. control, ** $p < 0.01$ vs. control, # $p < 0.01$ IL-1β +TNF-α vs. IL-1β. **B)** IL-1β decreases RCLMC tonic contractility in a dose dependent fashion. n= 6, *** $p < 0.001$ vs. control, ** $p < 0.01$ vs. control, * $p < 0.05$ vs. control, # p < 0.01 IL-1β (20 ng/ml) vs. IL-1β (10 ng/ml), *$ $p < 0.01$ IL-1β (20 ng/ml) vs. IL-1β (5 ng/ml). One-way ANOVA, with Bonferroni's post-hoc test; data are mean ±SEM.

Figure 4. IL-1β alone or IL-1β + TNF-α induced COX-2 expression in RCLMC, which was suppressed by Anakinra. **A)** RCLMC were treated with IL-1β, TNF-α, IL-1β + TNF-α , in the presence or absence of Anakinra for 24 hours (h). Equivalent amounts of total cell protein were subjected to Western blot analysis with antibodies against COX-2 and α-actin. **B)** The density of COX-2 bands was quantified. IL-1β treated RCLMC increased COX-2 protein levels significantly ($p < 0.01$), while TNF-α had no effect on COX-2 compared with control. TNF-α combined with IL-1β induced a higher-induction of COX-2 levels compared with IL-1β alone. Anakinra blocked the increased level of COX-2 induced by IL-1β alone or IL-1β + TNF-α after 24 h of treatment. n= 3, *** $p < 0.001$ vs. control, ** $p < 0.01$ vs. control, # $p < 0.01$ IL-1β +TNF-α vs. IL-1β alone. One-way ANOVA, with Bonferroni's post-hoc test; data are mean ±SEM.

Figure 5. COX-2 inhibition blocked IL-1β-induced RCLMC relaxation. **A)** COX-2 inhibition by both the nonselective COX-1/2 inhibitor (diclofenac) and the selective COX-2 inhibitor (Dup-697) blocked the IL-1β-induced RCLMC relaxation. On the other hand, the selective COX-1 inhibitor (TFAP) had no effect on IL-1β-induced RCLMC relaxation. **B)** None of COX inhibitor

treatments alone, (diclofenac, Dup-697 or TFAP), showed any significant effects on RCLMC contractility compared with control treatment. n= 6, ** $p < 0.01$ vs. control. One-way ANOVA, with Bonferroni's post-hoc test; data are mean ±SEM.

Figure 6. IL-1β dose dependently induced PGE_2 production in RCLMC, while EP4 receptor antagonist blocked IL-1β-induced RCLMC relaxation. **A)** IL-1β significantly increased PGE_2 production in RCLMC in a dose-dependent fashion (5-20ng/ml) compared with controls, while Anakinra blocked PGE_2 induction in RCLMC after 24 h of IL-1β (20ng/ml) treatment. TNF-α alone (20ng/ml) showed no significant effect on PGE_2 production in RCLMC. n= 3, *** $p < 0.001$ vs. control, ** $p < 0.01$ vs. control, * $p < 0.05$ vs. control, # $p < 0.01$ IL-1β (20 ng/ml) vs. IL-1β (10 ng/ml), $ $p < 0.01$ IL-1β (20 ng/ml) vs. IL-1β (5 ng/ml). **B)** EP4 receptor antagonist (GW627368X, 10^{-7}M and 10^{-6}M) blocked IL-1β (20ng/ml) induced RCLMC relaxation. PGE_2 treatment alone also induced RCLMC relaxation, while Anakinra–treatment showed no significant effect on the PGE_2-induced RCLMC relaxation. n= 5, ** $p < 0.01$ vs. control. One-way ANOVA, with Bonferroni's post-hoc test; data are mean ±SEM.

Figure 7. Diagram of cardiac lymphatic contraction disturbances in myocarditis. Dysfunction of lymphatic flow may occur in myocarditis in response to inflammatory cytokines including IL-1β and TNF-α. Prolonged expression and accumulation of inflammatory cytokines play a role in driving the progression from acute myocarditis into dilated cardiomyopathy (DCM) via failure of cardiac lymphatic pump to clear these inflammatory cells and their evolved cytokine. In acute myocarditis accumulation of these cytokines leads to a vicious cycle of inflammation and lymphostasis (insufficient lymphangion contractility) which exacerbates tissue damage and

DCM. IL-1β and IL-1β+TNF-α exert a profound depressant effect on cardiac lymphatic muscular contractility via COX-2 mediated PGE_2 production and EP4 receptor activation in an autocrine fashion to inhibit tonic contraction in an endothelial independent mechanism.

Established effects of IL-1β / IL-1β+TNF-α are shown as dashed lines. COX-2, cyclooxygenase-2; PGE_2, prostaglandin E 2; EP4, prostaglandin E receptor 4.

Table 1. Changes in genes expression in viral myocarditis (day 7)

Trivial gene name (*gene symbol*)	**Fold change**	***P* value**
IL-1β (*Il1b*)***	2.2	0.001
TNF-α (*Tnf*)***	2.06	0.001
IFN-γ (*Ifng*)***	2.36	0.001
COX-1 (*Ptgs1*)**	0.77	0.01
COX-2 (*Ptgs2*)***	2.17	0.001
IL-1 receptor 1 (*Il1r1*)	1.05	0.55
EP1 (*Ptgsr1*)	0.99	0.83
EP2 (*Ptgsr2*)	1.12	0.10
EP3 (*Ptgsr3*)	0.95	0.75
EP4 (*Ptgsr4*)***	1.39	0.001
LYVE-1 (*Lyve1*)	0.91	0.32
VEGFR3 (*Flt4*)	0.95	0.15

Levels of inflammatory mediator genes measured in heart tissue from control mice and mice with TMEV acute myocarditis.
n= 5, *** $P < 0.001$ vs. control, ** $P < 0.01$ vs. control. Student's *t*-test; data are mean

Table 1. Levels of inflammatory mediator genes measured in heart tissue from control mice and mice with TMEV acute myocarditis. n= 5, *** $p < 0.001$ vs. control, ** $p < 0.01$ vs. control. Student's *t*-test; data are mean ± standard error of the mean (SEM).

References

1. Martinez, N. E., F. Sato, E. Kawai, S. Omura, R. P. Chervenak, and I. Tsunoda. 2012. Regulatory T cells and Th17 cells in viral infections: implications for multiple sclerosis and myocarditis. *Future Virol* 7: 593-608.
2. Kearney, M. T., J. M. Cotton, P. J. Richardson, and A. M. Shah. 2001. Viral myocarditis and dilated cardiomyopathy: mechanisms, manifestations, and management. *Postgrad Med J* 77: 4-10.
3. Magnani, J. W., and G. W. Dec. 2006. Myocarditis: current trends in diagnosis and treatment. *Circulation* 113: 876-890.
4. Fabre, A., and M. N. Sheppard. 2006. Sudden adult death syndrome and other non-ischaemic causes of sudden cardiac death. *Heart* 92: 316-320.
5. Gavin, J. B., L. Maxwell, and S. G. Edgar. 1998. Microvascular involvement in cardiac pathology. *J Mol Cell Cardiol* 30: 2531-2540.
6. Miller, A. J. 1982. *Lymphatics Of The Heart*.
7. Shimada, T., T. Noguchi, K. Takita, H. Kitamura, and M. Nakamura. 1989. Morphology of lymphatics of the mammalian heart with special reference to the architecture and distribution of the subepicardial lymphatic system. *Acta Anat (Basel)* 136: 16-20.
8. Negrini, D., A. Moriondo, and S. Mukenge. 2004. Transmural pressure during cardiogenic oscillations in rodent diaphragmatic lymphatic vessels. *Lymphat Res Biol* 2: 69-81.
9. Zawieja, D. C., K. L. Davis, R. Schuster, W. M. Hinds, and H. J. Granger. 1993. Distribution, propagation, and coordination of contractile activity in lymphatics. *Am J Physiol* 264: H1283-1291.

10. Davis, M. J., A. M. Davis, C. W. Ku, and A. A. Gashev. 2009. Myogenic constriction and dilation of isolated lymphatic vessels. *Am J Physiol Heart Circ Physiol* 296: H293-302.
11. Souza-Smith, F. M., K. M. Kurtz, P. E. Molina, and J. W. Breslin. 2010. Adaptation of mesenteric collecting lymphatic pump function following acute alcohol intoxication. *Microcirculation* 17: 514-524.
12. Miller, A. J. 1982. *Lymphatics Of The Heart*.
13. Kampmeier, O. F. 1928. On the lymph flow of the human heart, with reference to the development of the channels and the first appearance, distribution, and physiology of their valves. *American Heart Journal* 4: 210-222.
14. Miller, A. J. 1982. *Lymphatics Of The Heart*.
15. Ullal, S. R., T. H. Kluge, and F. Gerbode. 1972. Studies on cardiac lymph during extracorporeal circulation. *Chest* 61: 662-667.
16. Taira, A., M. Yamashita, K. Arikawa, Y. Hamada, H. Toyohira, and H. Akita. 1979. Cardia lymph in electrical ventricular fibrillation: an experimental study. *Ann Thorac Surg* 27: 144-147.
17. Cui, Y. 2010. The role of lymphatic vessels in the heart. *Pathophysiology* 17: 307-314.
18. Witte, M. H., A. E. Dumont, R. H. Clauss, B. Rader, N. Levine, and E. S. Breed. 1969. Lymph circulation in congestive heart failure: effect of external thoracic duct drainage. *Circulation* 39: 723-733.
19. Dashkevich, A., C. Hagl, F. Beyersdorf, A. I. Nykanen, and K. B. Lemstrom. 2015. VEGF Pathways in the Lymphatics of Healthy and Diseased Heart. *Microcirculation*.

20. Zagrosek, A., R. Wassmuth, H. Abdel-Aty, A. Rudolph, R. Dietz, and J. Schulz-Menger. 2008. Relation between myocardial edema and myocardial mass during the acute and convalescent phase of myocarditis--a CMR study. *J Cardiovasc Magn Reson* 10: 19.

21. Feldman, A. M., and D. McNamara. 2000. Myocarditis. *N Engl J Med* 343: 1388-1398.

22. Dashkevich, A., W. Bloch, A. Antonyan, H. Goebel, J. U. Fries, C. Schlensak, F. Beyersdorf, and H. J. Geissler. 2010. Immunohistochemical study of remodeling of myocardial lymphatic and blood microvascular structures in terminal heart failure: differences between ischemic and dilated cardiomyopathy. *Lymphology* 43: 110-117.

23. Wu, T. F., C. J. Carati, W. K. Macnaughton, and P. Y. von der Weid. 2006. Contractile activity of lymphatic vessels is altered in the TNBS model of guinea pig ileitis. *Am J Physiol Gastrointest Liver Physiol* 291: G566-574.

24. Becker, F., P. Yi, M. Al-Kofahi, V. C. Ganta, J. Morris, and J. S. Alexander. 2014. Lymphatic dysregulation in intestinal inflammation: new insights into inflammatory bowel disease pathomechanisms. *Lymphology* 47: 3-27.

25. Aldrich, M. B., and E. M. Sevick-Muraca. 2013. Cytokines are systemic effectors of lymphatic function in acute inflammation. *Cytokine* 64: 362-369.

26. Al-Kofahi, M., F. Becker, F. N. Gavins, M. D. Woolard, I. Tsunoda, Y. Wang, D. Ostanin, D. C. Zawieja, M. Muthuchamy, P. Y. von der Weid, and J. S. Alexander. 2015. IL-1beta reduces tonic contraction of mesenteric lymphatic muscle cells, with the involvement of cycloxygenase-2 and prostaglandin E2. *Br J Pharmacol* 172: 4038-4051.

27. Shioi, T., A. Matsumori, and S. Sasayama. 1996. Persistent expression of cytokine in the chronic stage of viral myocarditis in mice. *Circulation* 94: 2930-2937.

28. Kawai, C. 1999. From myocarditis to cardiomyopathy: mechanisms of inflammation and cell death: learning from the past for the future. *Circulation* 99: 1091-1100.

29. Mann, D. L. 2002. Inflammatory mediators and the failing heart: past, present, and the foreseeable future. *Circ Res* 91: 988-998.

30. Matsumori, A. 1996. Cytokines in myocarditis and cardiomyopathies. *Curr Opin Cardiol* 11: 302-309.

31. von der Weid, P. Y., S. Rehal, and J. G. Ferraz. 2011. Role of the lymphatic system in the pathogenesis of Crohn's disease. *Curr Opin Gastroenterol* 27: 335-341.

32. Omura, S., E. Kawai, F. Sato, N. E. Martinez, G. V. Chaitanya, P. A. Rollyson, U. Cvek, M. Trutschl, J. S. Alexander, and I. Tsunoda. 2014. Bioinformatics multivariate analysis determined a set of phase-specific biomarker candidates in a novel mouse model for viral myocarditis. *Circ Cardiovasc Genet* 7: 444-454.

33. Sato, F., S. Omura, E. Kawai, N. E. Martinez, M. M. Acharya, P. C. Reddy, G. V. Chaitanya, J. S. Alexander, and I. Tsunoda. 2014. Distinct kinetics of viral replication, T cell infiltration, and fibrosis in three phases of myocarditis following Theiler's virus infection. *Cell Immunol* 292: 85-93.

34. Omura, S., E. Koike, and T. Kobayashi. 2009. Microarray analysis of gene expression in rat alveolar epithelial cells exposed to fractionated organic extracts of diesel exhaust particles. *Toxicology* 262: 65-72.

35. Jolliffe, I. T. 2011. *Principal Component Analysis*. New York: Springer. Briefings in bioinfomatics.

36. R Core Team (2015). R: A language and environment for statistical computing. . R Foundation for Statistical Computing, Vienna, Austria.

37. Chaitanya, G. V., S. Omura, F. Sato, N. E. Martinez, A. Minagar, M. Ramanathan, B. W. Guttman, R. Zivadinov, I. Tsunoda, and J. S. Alexander. 2013. Inflammation induces neuro-lymphatic protein expression in multiple sclerosis brain neurovasculature. *J Neuroinflammation* 10: 125.

38. Lee, C. S., W. F. Patton, N. Chung-Welch, E. T. Chiang, K. H. Spofford, and D. Shepro. 1998. Selective propagation of retinal pericytes in mixed microvascular cell cultures using L-leucine-methyl ester. *Biotechniques* 25: 482-488, 490-482, 494.

39. Muthuchamy, M., A. Gashev, N. Boswell, N. Dawson, and D. Zawieja. 2003. Molecular and functional analyses of the contractile apparatus in lymphatic muscle. *FASEB J* 17: 920-922.

40. Rasband, W. S. 1997-2012. ImageJ, U. S. National Institutes of Health, Bethesda, Maryland, USA, http://rsb.info.nih.gov/ij/.

41. Beasley, D. 1999. COX-2 and cytosolic PLA2 mediate IL-1beta-induced cAMP production in human vascular smooth muscle cells. *Am J Physiol* 276: H1369-1378.

42. Vigano, T., A. Habib, A. Hernandez, A. Bonazzi, D. Boraschi, M. Lebret, E. Cassina, J. Maclouf, A. Sala, and G. Folco. 1997. Cyclooxygenase-2 and synthesis of PGE2 in human bronchial smooth-muscle cells. *Am J Respir Crit Care Med* 155: 864-868.

43. Silver, M. A., and D. Kowalczyk. 1989. Coronary microvascular narrowing in acute murine coxsackie B3 myocarditis. *Am Heart J* 118: 173-174.

44. Factor, S. M., T. Minase, S. Cho, R. Dominitz, and E. H. Sonnenblick. 1982. Microvascular spasm in the cardiomyopathic Syrian hamster: a preventable cause of focal myocardial necrosis. *Circulation* 66: 342-354.

45. Yilmaz, A., H. Mahrholdt, A. Athanasiadis, H. Vogelsberg, G. Meinhardt, M. Voehringer, E. M. Kispert, C. Deluigi, H. Baccouche, E. Spodarev, K. Klingel, R. Kandolf, and U. Sechtem. 2008. Coronary vasospasm as the underlying cause for chest pain in patients with PVB19 myocarditis. *Heart* 94: 1456-1463.

46. Crea, F., P. G. Camici, and C. N. Bairey Merz. 2014. Coronary microvascular dysfunction: an update. *Eur Heart J* 35: 1101-1111.

47. Yamada, T., A. Matsumori, and S. Sasayama. 1994. Therapeutic effect of anti-tumor necrosis factor-alpha antibody on the murine model of viral myocarditis induced by encephalomyocarditis virus. *Circulation* 89: 846-851.

48. Lane, J. R., D. A. Neumann, A. Lafond-Walker, A. Herskowitz, and N. R. Rose. 1992. Interleukin 1 or tumor necrosis factor can promote Coxsackie B3-induced myocarditis in resistant B10.A mice. *J Exp Med* 175: 1123-1129.

49. Park, J. H., J. Y. Yoon, S. M. Ko, S. A. Jin, J. H. Kim, C. H. Cho, J. M. Kim, J. H. Lee, S. W. Choi, I. W. Seong, and J. O. Jeong. 2011. Endothelial progenitor cell transplantation decreases lymphangiogenesis and adverse myocardial remodeling in a mouse model of acute myocardial infarction. *Exp Mol Med* 43: 479-485.

50. Klotz, L., S. Norman, J. M. Vieira, M. Masters, M. Rohling, K. N. Dube, S. Bollini, F. Matsuzaki, C. A. Carr, and P. R. Riley. 2015. Cardiac lymphatics are heterogeneous in origin and respond to injury. *Nature* 522: 62-67.

51. Benvenuti, L. A., A. M. Silva, and V. D. Aiello. 2010. [Quantification of lymphatic vessels in dilated and chronic chagasic cardiomyopathy]. *Arq Bras Cardiol* 94: 564-567.

52. Laine, G. A., and S. J. Allen. 1991. Left ventricular myocardial edema. Lymph flow, interstitial fibrosis, and cardiac function. *Circ Res* 68: 1713-1721.

53. Chaitanya, G. V., S. E. Franks, W. Cromer, S. R. Wells, M. Bienkowska, M. H. Jennings, A. Ruddell, T. Ando, Y. Wang, Y. Gu, M. Sapp, J. M. Mathis, P. A. Jordan, A. Minagar, and J. S. Alexander. 2010. Differential cytokine responses in human and mouse lymphatic endothelial cells to cytokines in vitro. *Lymphat Res Biol* 8: 155-164.

54. Beasley, D., R. A. Cohen, and N. G. Levinsky. 1989. Interleukin 1 inhibits contraction of vascular smooth muscle. *J Clin Invest* 83: 331-335.

55. Beasley, D., and M. Eldridge. 1994. Interleukin-1 beta and tumor necrosis factor-alpha synergistically induce NO synthase in rat vascular smooth muscle cells. *Am J Physiol* 266: R1197-1203.

56. Fearon, W. F., and D. T. Fearon. 2008. Inflammation and cardiovascular disease: role of the interleukin-1 receptor antagonist. *Circulation* 117: 2577-2579.

57. Ikonomidis, I., J. P. Lekakis, M. Nikolaou, I. Paraskevaidis, I. Andreadou, T. Kaplanoglou, P. Katsimbri, G. Skarantavos, P. N. Soucacos, and D. T. Kremastinos. 2008. Inhibition of interleukin-1 by anakinra improves vascular and left ventricular function in patients with rheumatoid arthritis. *Circulation* 117: 2662-2669.

58. Garat, C., and W. P. Arend. 2003. Intracellular IL-1Ra type 1 inhibits IL-1-induced IL-6 and IL-8 production in Caco-2 intestinal epithelial cells through inhibition of p38 mitogen-activated protein kinase and NF-kappaB pathways. *Cytokine* 23: 31-40.

59. Gui, Y., X. L. Zheng, and M. D. Hollenberg. 2000. Interleukin-1beta, Src- and non-Src tyrosine kinases, and nitric oxide synthase induction in rat aorta in vitro. *Am J Physiol Heart Circ Physiol* 279: H566-576.

60. Nakano, A., A. Matsumori, S. Kawamoto, H. Tahara, E. Yamato, S. Sasayama, and J. I. Miyazaki. 2001. Cytokine gene therapy for myocarditis by in vivo electroporation. *Hum Gene Ther* 12: 1289-1297.

61. Takahashi, T., S. J. Zhu, H. Sumino, S. Saegusa, T. Nakahashi, K. Iwai, S. Morimoto, and T. Kanda. 2005. Inhibition of cyclooxygenase-2 enhances myocardial damage in a mouse model of viral myocarditis. *Life Sci* 78: 195-204.

62. Steer, S. A., J. M. Moran, L. B. Maggi, Jr., R. M. Buller, H. Perlman, and J. A. Corbett. 2003. Regulation of cyclooxygenase-2 expression by macrophages in response to double-stranded RNA and viral infection. *J Immunol* 170: 1070-1076.

63. Blirando, K., R. Blaise, N. Gorodnaya, C. Rouxel, O. Meilhac, P. Vincent, and I. Limon. 2015. The stellate vascular smooth muscle cell phenotype is induced by IL-1beta via the secretion of PGE2 and subsequent cAMP-dependent protein kinase A activation. *Biochim Biophys Acta* 1853: 3235-3247.

64. Davis, M. J., E. Rahbar, A. A. Gashev, D. C. Zawieja, and J. E. Moore, Jr. 2011. Determinants of valve gating in collecting lymphatic vessels from rat mesentery. *Am J Physiol Heart Circ Physiol* 301: H48-60.

65. Alitalo, K. 2011. The lymphatic vasculature in disease. *Nat Med* 17: 1371-1380.

66. Omura S, Kawai E, Sato F, Martinez NE, Chaitanya GV, Rollyson PA, Cvek U, Trutschl M, Alexander JS, Tsunoda I. Bioinformatics multivariate analysis determined a set of phase-specific biomarker candidates in a novel mouse model for viral myocarditis. Circ Cardiovasc Genet. 2014 Aug;7(4):444-54.

67. Baskar S, Klein AL, Zeft A. The Use of IL-1 Receptor Antagonist (Anakinra) in Idiopathic Recurrent Pericarditis: A Narrative Review. Cardiology Research and Practice. 2016;2016:78, 40724. doi:10.1155/2016/7840724.

Figure 1

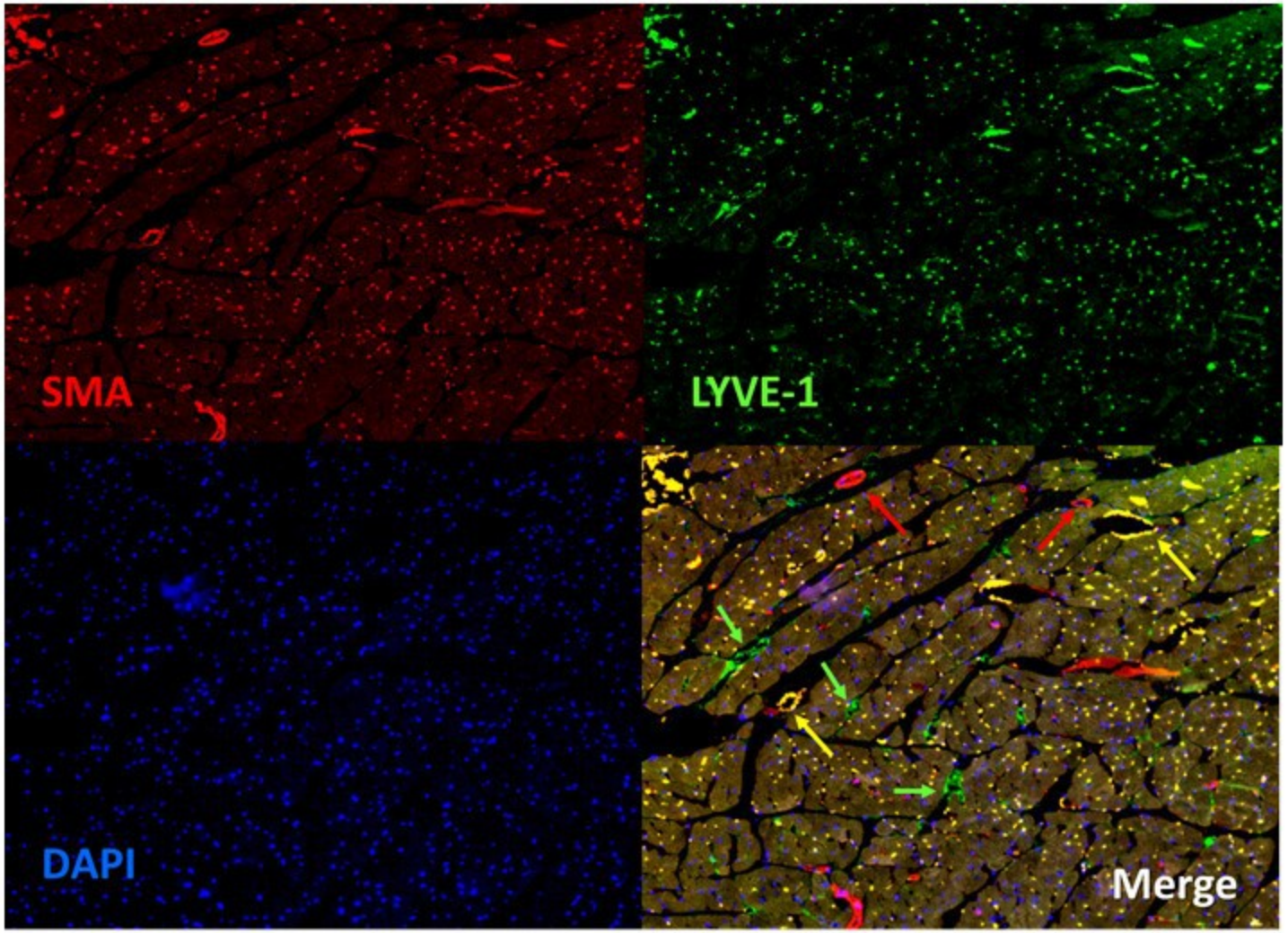

Figure 2

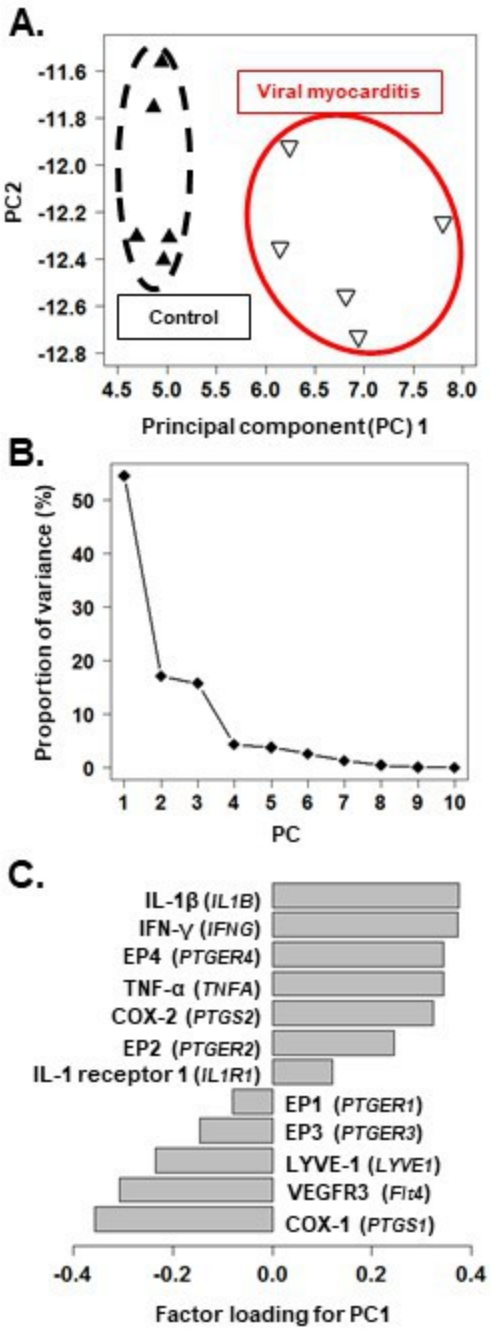
A.
Viral myocarditis
Control
PC2
-11.6
-11.8
-12.0
-12.2
-12.4
-12.6
-12.8
4.5 5.0 5.5 6.0 6.5 7.0 7.5 8.0
Principal component (PC) 1
B.
Proportion of variance (%)
50
40
30
20
10
0
1 2 3 4 5 6 7 8 9 10
PC
C.
IL-1β (IL1B)
IFN-γ (IFNG)
EP4 (PTGER4)
TNF-α (TNFA)
COX-2 (PTGS2)
EP2 (PTGER2)
IL-1 receptor 1 (IL1R1)
EP1 (PTGER1)
EP3 (PTGER3)
LYVE-1 (LYVE1)
VEGFR3 (Flt4)
COX-1 (PTGS1)
-0.4 -0.2 0.0 0.2 0.4
Factor loading for PC1

Figure 3

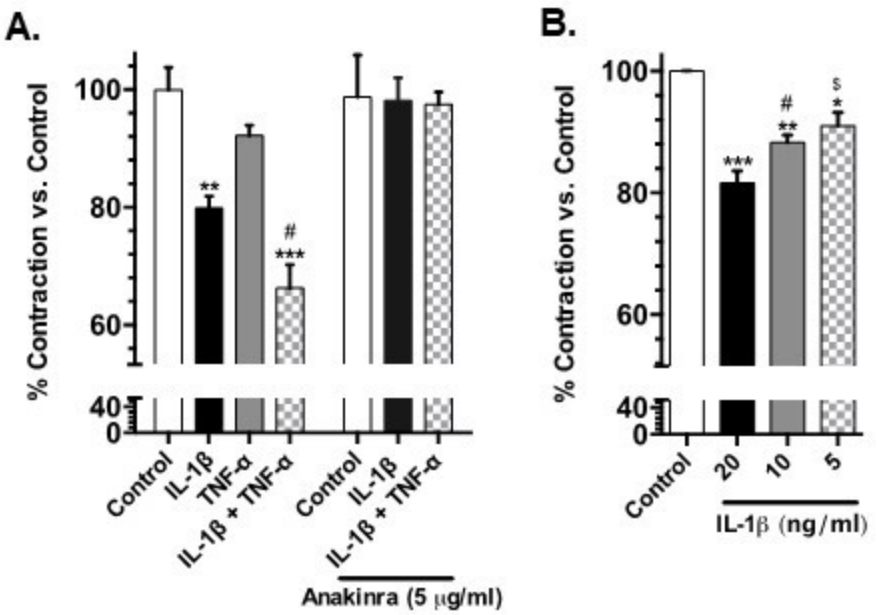
A.
% Contraction vs. Control
100
80
60
40
0
**
#
***
Control
IL-1β
TNF-α
IL-1β + TNF-α
Control
IL-1β
IL-1β + TNF-α
Anakinra (5 μg/ml)
B.
% Contraction vs. Control
100
80
60
40
0
***
#
**
$
*
Control
20
10
5
IL-1β (ng/ml)

Figure 4

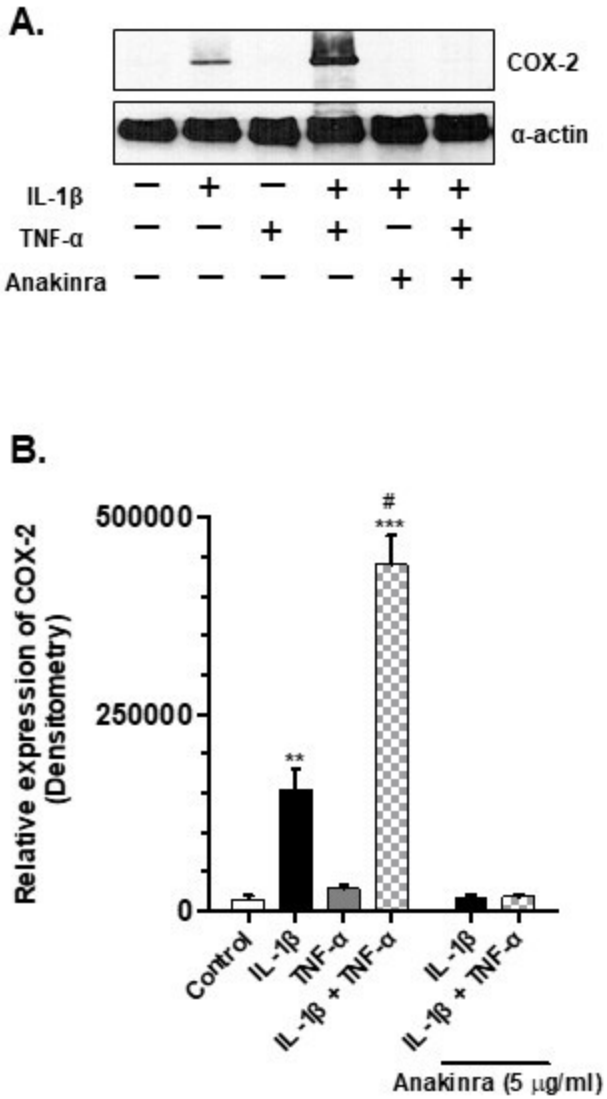
A.
COX-2
α-actin
IL-1β
TNF-α
Anakinra
B.
Relative expression of COX-2 (Densitometry)
500000
250000
0
**
#
***
Control
IL-1β
TNF-α
IL-1β + TNF-α
IL-1β
IL-1β + TNF-α
Anakinra (5 μg/ml)

Figure 5

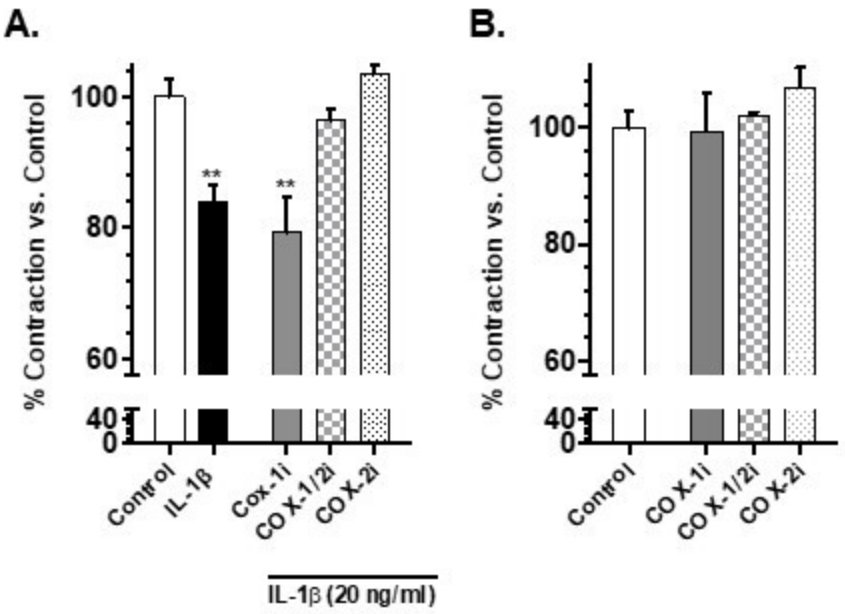
A.
B.
% Contraction vs. Control
100
80
60
40
0
**
**
Control
IL-1β
Cox-1i
COX-1/2i
COX-2i
IL-1β (20 ng/ml)

Figure 6

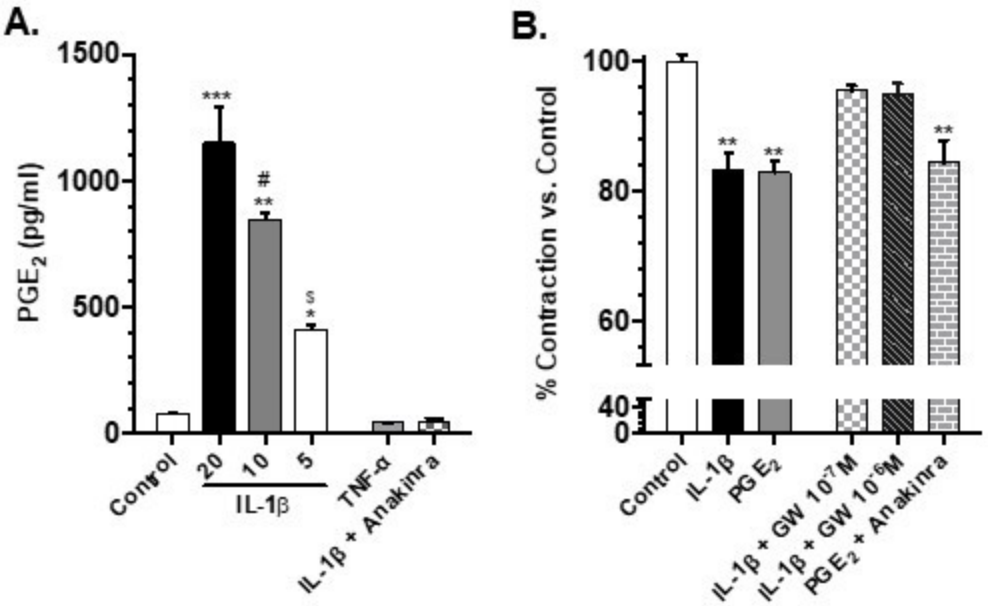
A.
1500
1000
500
0
PGE2 (pg/ml)
***
**
#
**
Control
20
10
5
IL-1β
TNF-α
IL-1β + Anakinra
B.
100
80
60
40
0
% Contraction vs. Control
**
**
**
Control
IL-1β
PGE2
IL-1β + GW 10-7M
IL-1β + GW 10-6M
PGE2 + Anakinra

Figure 7

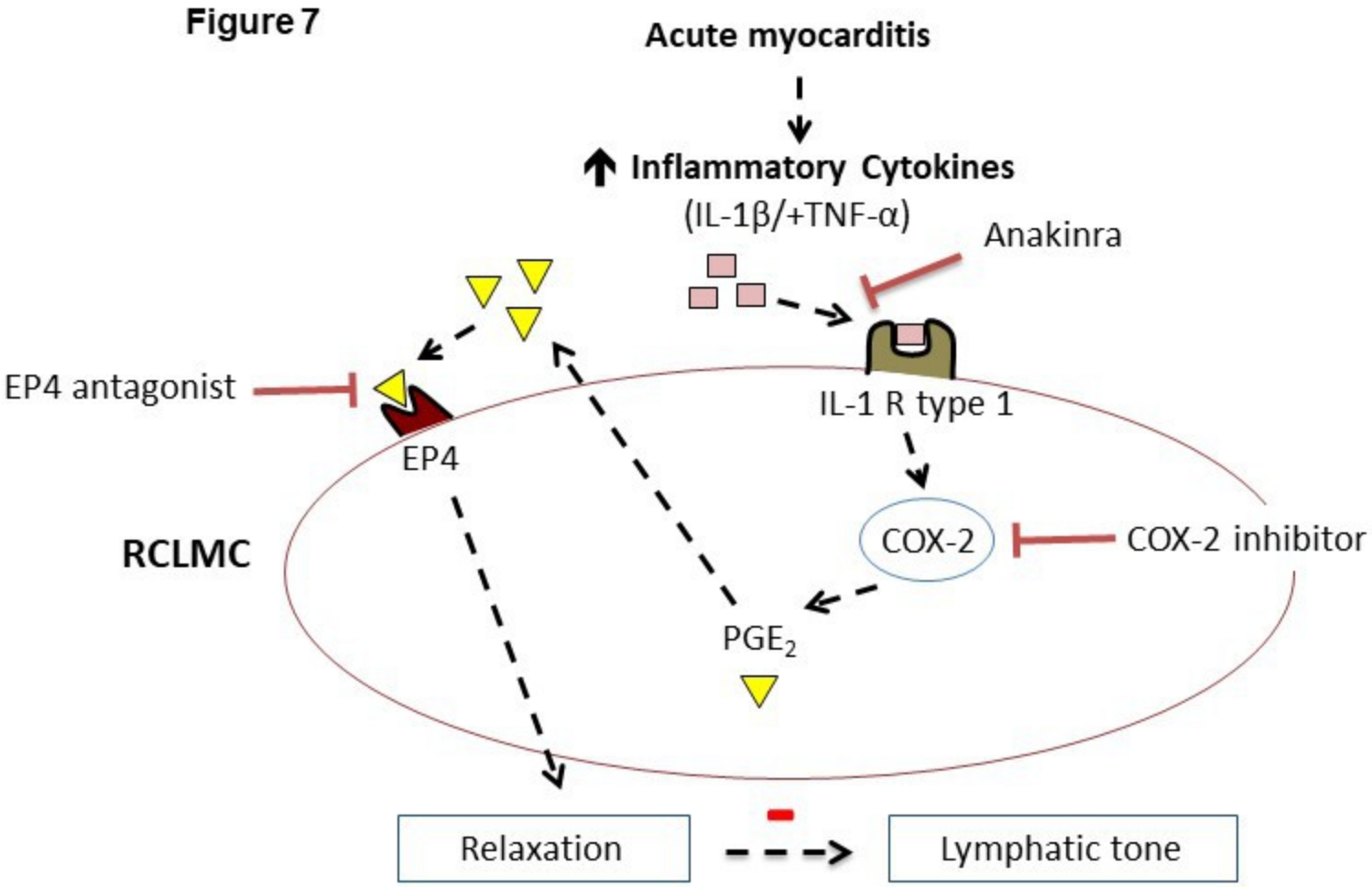
Acute myocarditis
Inflammatory Cytokines
(IL-1β/+TNF-α)
Anakinra
EP4 antagonist
IL-1 R type 1
EP4
RCLMC
COX-2
COX-2 inhibitor
PGE2
Relaxation
Lymphatic tone